Assessing the potential of using telecommunication microwave links in urban drainage modelling

M. Fencl, J. Rieckermann, M. Schleiss, D. Stránský and V. Bareš

Martin Fencl, Czech Technical University in Prague, Department of Hydraulics and Hydrology, Thákurova 7, 165 00 Prague 6, Czech Republic (martin.fencl@fsv.cvut.cz)
Jörg Rieckermann, Eawag: Swiss Federal Institute of Aquatic Science and Technology, Department of Urban Water Management, Überlandstrasse 133, 8600 Dübendorf, Switzerland
Marc Schleiss, École Polytechnique Fédérale de Lausanne (EPFL), Laboratoire de Télédétection Environnementale (LTE), Bâtiment GR, Station 2, CH-1015 Lausanne, Switzerland
David Stránský, Czech Technical University in Prague, Department of Sanitary and Ecological Engineering, Thákurova 7, 165 00 Prague 6, Czech Republic
Vojtěch Bareš, Czech Technical University in Prague, Department of Hydraulics and Hydrology, Thákurova 7, 165 00 Prague 6, Czech Republic and UCEEB CTU Nam. Sitna 3105, 272 01 Kladno 2, Czech Republic

ABSTRACT

The ability to predict the runoff response of an urban catchment to rainfall is crucial for managing drainage systems effectively and controlling discharges from urban areas. In this paper we assess the potential of commercial microwave links (MWL) to capture the spatio-temporal rainfall dynamics and thus improve urban rainfall-runoff modelling. Specifically, we perform numerical experiments with virtual rainfall fields and compare the results of MWL rainfall reconstructions to those of rain gauge (RG) observations. In a case study, we are able to show that MWL networks in urban areas are sufficiently dense to provide good information on spatio-temporal rainfall variability and can thus considerably improve pipe flow prediction, even in small subcatchments. In addition, the better spatial coverage also improves the control of discharges from urban areas. This is especially beneficial for heavy rainfall, which usually has a high spatial variability that cannot be accurately captured by RG point measurements.

KEYWORDS

urban drainage modeling; telecommunication microwave links; rainfall estimation; space-time structure; input uncertainty

INTRODUCTION

The ability to predict the hydrologic response of an urban catchment to rainfall, and thus to control discharges from urban areas, requires high-quality rainfall data. For urban rainfall data, a high spatial as well as a high temporal resolution are mandatory because urban subcatchments are relatively small and runoff is generated extremely fast on impervious surfaces.

This document is the accepted manuscript version of the following article:
Fencl, M., Rieckermann, J., Schleiss, M., Stránský, D., & Bareš, V. (2013). Assessing the potential of using telecommunication microwave links in urban drainage modelling. Water Science and Technology, 68(8), 1810-1818. https://doi.org/10.2166/wst.2013.429

Conventional rain gauges (RG) can provide the necessary temporal resolution. However, as a point measurement they cannot capture the rainfall spatial variability adequately (Berne et al. 2004). The maintenance of a dense RG network is very costly and local weather radars (LAWR) are not often available. In addition, LAWR estimations are affected by many uncertainties (Thorndahl and Rasmussen 2012). C-band country-wide weather radars are usually available, but their resolution (rarely finer than 1 x 1 km^2 and 5 min) and data quality is often not sufficient for many urban drainage tasks.

Commercial microwave links (MWL) are a novel source of rainfall information which could bridge this gap. They operate at frequencies where raindrops are the dominant source of microwave attenuation. This attenuation can be calculated from the difference between received signal levels with and without rainfall and can be transformed to the path-averaged rain rate (Messer et al. 2006, Leijnse et al. 2007). Using MWL in urban drainage modelling is conceptually interesting because MWL networks *i)* are already built and could provide rainfall information at virtually no additional cost, *ii)* observe near-surface precipitation a few tens of meters above ground, and *iii)* have a high density in urban areas (Rieckermann et al. 2009). In addition, MWL provide path-averaged rain rates over distances ranging from a few hundred meters to a few kilometers. Thus, the spatial resolution of MWL observations very well matches the scale of urban subcatchments. Although the theory behind the MWL rainfall estimation is quite well understood, there are few hydrological applications (Overeem et al. 2011, Fenicia et al. 2012). Studies which use MWL for rainfall-runoff modelling in an urban setting are currently lacking.

In this manuscript, we therefore investigate how data from commercial telecommunication networks can improve urban drainage modelling. Specifically, we analyze the extent to which better information about spatio-temporal rainfall variability improves pipe flow predictions. To this aim, we perform computational experiments that allow us to compare MWL to RG measurements for several realizations of exactly known reference rainfall, which is not possible with incomplete real-world observations. To avoid overconfidence in the results, we explicitly consider the uncertainties associated with the different sensor types. Our analysis for a suburb of Prague, Czech Republic, suggests that MWL networks in urban areas are sufficiently dense to provide good information on spatio-temporal rainfall variability.
In the future, when the infrastructure to acquire MWL data from telecommunication operators is fully implemented, we will validate our results with real-world data.

METHODS AND MATERIAL

To assess the potential of using MWL in urban drainage modelling, we compare runoff predictions from MWL to those using RG observations using the rainfall-runoff model of a case study area located in Letňany, a suburb of Prague, Czech Republic. The analysis is based on virtual drop size distribution (DSD) fields, which not only enable us to estimate rain rates at any location, but also to calculate the expected rain-induced attenuation for a particular MWL (Schleiss et. al 2012). Thus we can reliably simulate the reference rain rates fallen over the catchment and extract point rain rates as seen by RG as well as path-averaged rain rates as seen by MWL. To avoid overconfidence, we perturb the virtual data with realistic observation errors for both RG and MWL measurements. These are then propagated through a hydrodynamic rainfall-runoff model of a case study catchment with Monte Carlo simulations for all rainfall datasets.

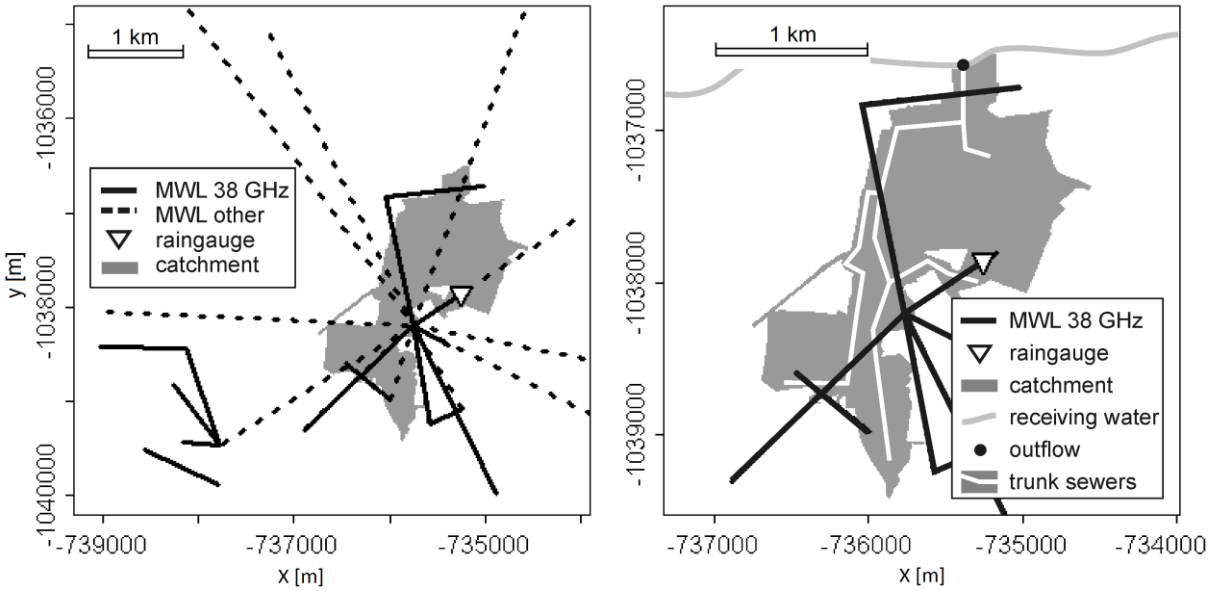

Figure 1 Left: Study catchment and MWL network: the links displayed by the solid line were used for the rainfall spatial reconstruction. Right: Disposition of trunk sewers of the catchment: flow conditions were evaluated at the outlet from the catchment depicted by black point.

The case study catchment has an area of 2.33 km^2, with an impervious area of about 64 %, which is drained by a separate sewer system (Figure 1). The Prague urban area is covered by a dense network of many hundred MWL. For the rainfall spatial reconstruction we selected 14 MWL (MINI-LINK, Ericsson, owned by T-Mobile) which are located in the direct vicinity of the catchment and operate at frequencies of around 38 GHz, which have an almost linear response to rainfall and are therefore most convenient for rainfall estimation. Regarding the RG measurement, we copied the experimental set-up with a single RG that was deployed by the sewer operator in their monitoring study to validate the rainfall-runoff model (Figure 1).

Reference rainfall fields

The reference areal rain rates are simulated using a virtual drop size distribution (DSD) generator (Schleiss et al., 2012), which is based on geostatistics and can generate intermittent DSD fields in space and time with realistic structures. The DSD *N(D)* provides information about the average number of drops with equivolume spherical drop diameter *D* [mm] per unit volume of atmosphere. It is a combination of a concentration parameter N_t [m^{-3}] and probability density function (PDF) *f(D)*:

$$N(D) = N_t f(D) \quad (1)$$

In the simulation, *f(D)* represents the density of a Gamma distribution with two parameters: μ [-] and Λ [mm^{-1}]. The generator estimates the medium and large scale rainfall variability (1 - 50 km) together with advection direction and velocity using radar data. The small scale variability (0.1-1 km) of the DSD is parameterized based on disdrometer data collected in Lausanne, Switzerland. The DSD fields are sampled every 1 minute and have a spatial resolution of 0.1 x 0.1 km^2. The original size of a DSD field is 20 x 20 km^2.

The DSD information can be transformed to the rain rate *R* [mm/h] at any location of a DSD field:

$$R = 6*10^{-4}\pi * \int_D N(D) * v(D) * D^3 dD \quad (2)$$

where *N(D)* is calculated according to (1) and *v(D)* [m/s] represents the terminal velocity of a rain drop with diameter *D* (Beard 1977, Berne and Uijlenhoet 2007).

As the response of the catchment fundamentally depends on the rainfall characteristics, we generated three rain events: The first is a heavy convective rainfall event with low intermittency and a duration of 30 min. The second has moderate convective rainfall of high intermittency and lasts 60 min. The last event has strong stratiform rainfall of low intermittency lasting 120 min.

To eliminate the influence of positioning the DSD field over the study area, the relative position of the catchment to the DSD fields was repeatedly changed to cover 25 different locations uniformly distributed over the field. This finally resulted in a comprehensive set of 75 reference areal rainfalls of size 7 x 7 km^2 with maximal point rain rates up to 50 mm/h and total heights up to 12 mm. From these, we extracted virtual RG data and computed MWL reconstructions.

RG and MWL observations

Virtual RG measurements are extracted from each of the 75 reference rainfalls at one particular cell of a rainfall field at each time step using (2). Because of the high spatial resolution of the reference rainfall (100 x 100 m^2), the representativeness error between the rain rate at the point scale and the simulated areal rain rate is assumed to be negligible.

The attenuation of the MWL signal caused by raindrops can be calculated using the T-Matrix method (Mishchenko and Travis 1998). Knowing the DSD along each particular link (by extracting it from the simulated DSD field), we can calculate the path-averaged specific attenuation *k* [dB/km] at any time step:

$$k = \frac{1}{\ln(10)} * \int_D \sigma(D,\lambda) * \overline{N}(D) * dD \quad (3)$$

The extinction cross-section $\sigma(D, \lambda)$ [cm^2] describes how a raindrop of diameter *D* attenuates a signal of wavelength λ and $\overline{N}(D)$ represents the average *N(D)* (1) of the cells of the simulated DSD field intersected by the link. The product of these magnitudes is integrated over the whole range of raindrop diameters and transformed by the logarithmic constant to decibels. A simple power law relation (4) is then used to transform the path-averaged specific attenuation *k* [dB/km] into the path-averaged rain rate *R* [mm/h] (Messer et al. 2006):

$$R = \alpha * k^{\beta} \quad (4)$$

Empirical parameters α and β are estimated for each link separately by fitting the power law estimated rain rate of all events to the path-averaged one retrieved directly from the DSD fields (2).

Measurement uncertainty

RG measurement uncertainties are modelled according to Stransky et al. (2007), who investigated the uncertainty of tipping bucket RG. Our RG is considered to be statically and dynamically calibrated. The uncertainties due to losses caused by wind, wetting and evaporation as well as owing to standard calibration procedures are sampled from PDFs with respect to the nature of the processes:

Wind losses are calculated according to Sevruk (1996) as a function of wind velocities considering velocities as log-normally distributed (mean = 2.078, sd = 0.639), which corresponds to typical Czech wind characteristics. Then, the wind losses are perturbed by a realistic measurement error sampled from a uniform PDF (± 1 % of unbiased rain rate). The error due to wetting is sampled for the first intervals of a rain event from a triangular PDF (mode = 2 - 10 % (sampled form uniform PDF), range: mode value ± 2 %). The evaporation losses are sampled from a triangular PDF (mode = 2 %, range: 0 % to 4 %). And finally the error due to calibration is sampled from a normal PDF (mean = 0, sd = 0.07 * unbiased rain rate (R_{rg})).

MWL rainfall estimates are affected by different sources of uncertainties. Most of the errors account for improper baseline determination, quantization noise, the power law approximation (4) and additional attenuation caused by antenna wetting (in the following referred to as "wet antenna effect") (Leijnse et al. 2008).

The uncertainty caused by quantization noise and baseline determination is regarded as normally distributed. It has been parameterized on a comprehensive dataset from a real-world case study in the greater Zurich area (Rieckermann et al. 2009; Fencl 2011). The uncertainty due to quantization noise and baseline separation is sampled for each MWL independently from a normal PDF (mean = 0, sd = 1/6 dB). As received signal levels of operational MWL typically have a quantization of 1 dB, we round the final attenuation to integer values. This also partly compensates for the fact that in this study we do not reproduce the wet antenna effect, which is subject to ongoing research (Kharadly and Ross 2001, Leijnse et al. 2008, Schleiss et al. 2013).

Rainfall reconstruction using MWL data

As a typical network contains MWLs of different lengths and orientations, the two-dimensional rainfall spatial variability can be reconstructed to some extent from the joint analysis of nearby MWL. For simplicity, we used the algorithm by Goldshtein et al. (2009). The algorithm first divides each MWL into equal subsections approximately 0.5 km long and iteratively estimates the rainfall distribution along each MWL, using rainfall information from neighboring MWL (Figure. 2). Second, it extrapolates the estimated rainfall intensities to a regular two-dimensional grid. We use 20 iterations as suggested by Goldshtein et al. (2009) and project rain rates onto the rectangular grid with resolution 0.25 x 0.25 km^2.

Rainfall-runoff simulations

To predict a realistic runoff response from the catchment to the different types of rainfall observations, we use a calibrated hydrodynamic model. The model of a Letňany suburb has been constructed for the urban drainage masterplan of Prague and has been implemented in the commercial solver MIKE URBAN with the MOUSE computational engine. The case study catchment is represented by 188 subcatchments defined according to the topology of the case study area. The surface runoff module uses the simple time-area method.

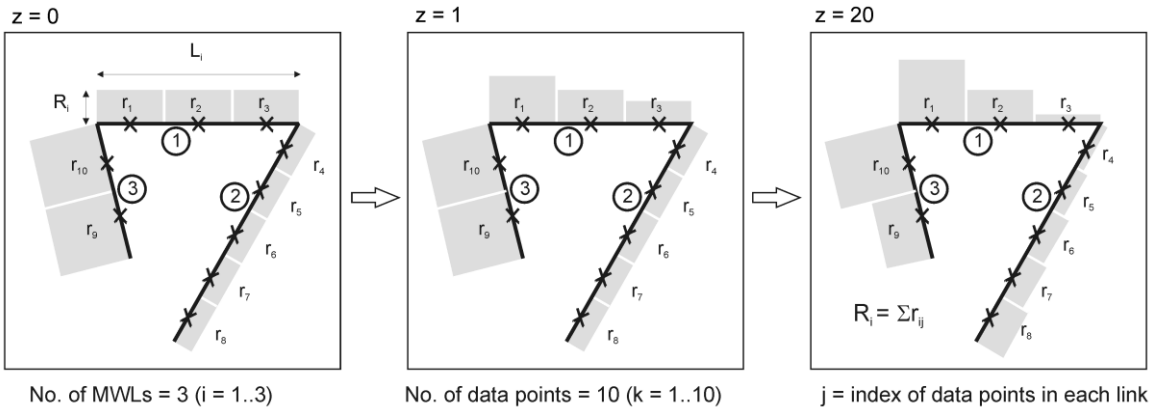

Figure 2 Illustration of rainfall reconstruction from the observations of three neighboring MWL. Left: Initial uniform distribution of rainfall among MWL subsections for a given MWL topology. Middle: Distribution estimated for a link ① in the first iteration (*z*). Right: The reconstructed rainfall distribution along the links after the last iteration (*z*).

Placing the reference and MWL reconstructed areal rainfalls over the catchment area, individual rainfall time series can be assigned to each subcatchment from cells of respective rainfall fields overlapping the particular subcatchment. When more cells belong to one subcatchment, the final rain rates are calculated as averages weighted by the area of cells overlapping the subcatchment. RG measurements, as they provide only point rainfall information, are regarded as one identical rainfall time series for all subcatchments.

Each of the 75 rain events results in one reference rainfall (with full rain rate spatial information) and 25 realizations of MWL reconstructed rainfall and 25 realizations of RG rainfall, where scatter of these multiple realizations arises from limited accuracy of MWL and RG respectively. Thus for the reference rainfall, which is known exactly, one runoff simulation per rain event is performed. For MWL and RG rainfall, the corresponding measurement errors are propagated by Monte Carlo simulations with $n = 25$ repetitions for each data set.

Performance assessment

To compare the MWL rainfall observations to RG data, we first compute relevant performance statistics for rainfall as well as pipe flow at the outfall from the catchment (Figure 1). We then compare them with those of the reference rainfall. For each rain event and realization (i.e., input data set for a rainfall-runoff simulation), we compute a) the peak areal rain rate (R_{max}), and b) the rainfall volume (RV), considering only those rainfall cells which are within the catchment area. From the corresponding runoff hydrograph we compute c) the peak flow (Q_{max}) and d) the outflow volume (QV) at the catchment outlet. For performance assessment, we use the relative error with regard to the reference rainfall and runoff values R_{max_ref}, RV_{ref} and Q_{max_ref}, QV_{ref} , respectively. Its mean represents the bias and its standard deviation the uncertainty due to both the limited spatial information and the limited precision of each measuring technique.

In addition, we also evaluate how closely the predicted runoff from each monitoring technique matches the runoff dynamics of the reference rainfall for each event and realization. Performance measures to reproduce the reference hydrograph are the mean absolute error (MAE) and root mean square error (RMSE), between reference and estimated values, the

latter being more sensitive to outliers. To ensure a fair comparison, we normalize both MAE and RMSE by a) the peak runoff rates from the reference rainfall (NMAE, resp. NRMSE):

$$NMAE = \frac{MAE}{Q_{\max\_ ref}} * 100 \quad (5)$$

$$NRMSE = \frac{RMSE}{Q_{\max\_ ref}} * 100 \quad (6)$$

and b) the mean flow rates (CV(MAE), resp. CV(RMSE)):

$$CV(MAE) = \frac{MAE}{Q_{mean\_ ref}} * 100 \quad (7)$$

$$CV(RMSE) = \frac{RMSE}{Q_{mean\_ ref}} * 100 \quad (8)$$

and express them in percent.

The ability to reproduce trends in the flow rates is evaluated by Pearson's correlation coefficient *r*.

To reveal the effect of a systematic temporal shift of runoff hydrographs, the performance statistics ((5-8) and *r*) are computed for the predicted flow shifted forward and backward in time against the reference runoff by one and two time steps.

To guarantee a realistic evaluation, only the events in the whole performance assessment that are relevant from an engineering viewpoint ($Q_{max,ref}$ > 10 l/s) and those that produce considerable peak runoff ($Q_{max,est}$ > 5 l/s) were considered. This was necessary because the runoff is very sensitive to small changes in model parameters (e.g., pipe roughness coefficients) and discharge predictions at such low flows are not robust.

RESULTS AND DISCUSSION

In general, we found that the ability to predict runoff dynamics of a storm event at spatial scales of a few square kilometers, as in our catchment, essentially depends on the correct estimation of areal rain rate and its temporal dynamics. In contrast, our results suggest that the correct spatial distribution of rainfall is less important.

Rainfall estimates

Regarding the spatio-temporal characteristics of the rainfall fields, we found that the MWL reconstructions from the path-averaged observations in general smooth out the local maxima and minima. Interestingly, although they are locally systematically biased, they capture the rain rates averaged over the whole area of the catchment very well (Table 1). In addition, they correctly identify the location of the peak rainfall rates. As we only consider uncertainties due to quantization noise, baseline separation and the power law relationship (4), the uncertainties

of MWL rainfall estimates are almost independent of rainfall rates because the parameter β of a power law (4) almost equals 1 at 38 GHz frequencies (Berne and Uijlenhoet 2007).

In contrast to MWL, RG can capture rain rate maxima and minima in its direct vicinity; however, the areal rain rate estimates are less reliable (Table 1). This applies especially to high rain rates because the spatial rainfall variability is in general higher during periods of heavy rainfall and RG, as a point measurement, cannot reflect the spatial distribution of rainfall. In addition, the precision of tipping bucket RG decreases with growing rain rate. Therefore, the areal rates of heavy rainfall are better reproduced by the MWL network, whereas with light rainfall the performance of both methods is comparable. Given the 1 dB quantization, this is a very promising result.

Table 1 Performance statistic of rainfall reconstruction (rainfall volumes and peak areal rainfalls) in comparison to the reference rainfall. The standard deviation is given in brackets.

	RV – mean rel. error	**R_{max} – mean rel. error**
RG	4 % (14 %)	34 % (27 %)
MWL	-3 % (10 %)	0 % (10 %)

Flow estimates

Regarding the performance to predict sewer discharges, the threshold for evaluating the rainfall induced flows ($Q_{max\ ref}$> 10 l/s and $Q_{max\ est}$> 5 l/s) was exceeded by 40 of the 75 rain events.

Runoff peaks and volumes: Although MWL-based predictions of runoff peaks and volumes have a larger bias than RG, this occurs mostly during periods of low or moderate flows, when large relative deviations are not critical in absolute values. In contrast to the bias, the standard deviation of the MWL results is considerably lower than that from RG (Table 2, Figure 3).

Table 2 Performance statistics of estimated peak flows and flow volumes to the reference values. The standard deviation is given in brackets.

	QV – mean rel. error	**Q_{max} – mean rel. error**
RG	6 % (26 %)	6 % (26 %)
MWL	-12 % (11 %)	-9 % (11 %)

Runoff dynamics: The comparison of hydrographs revealed that MWL-based predictions capture the pipe flow temporal dynamics better than RG estimates (Table 3, Figure 5, 6). Similar to outflow volume and peak flow predictions, the MWL perform better than RG during periods of high flows, i.e. during heavy rainfall (Figure 4, 5, 6). This is because for heavy rainfall the lack of spatial information by RG accounts for a higher rate of uncertainty than the limited precision of particular rain rate estimates from particular MWL. In contrast, during light rainfall the limited precision of MWL causes relatively high scatter in flow estimates in comparison to those from RG (Figure 4). However, since the MWL estimates are less biased on average than RG estimates, the accuracy of both methods is comparable for light rainfall. (Figure 5, 6)

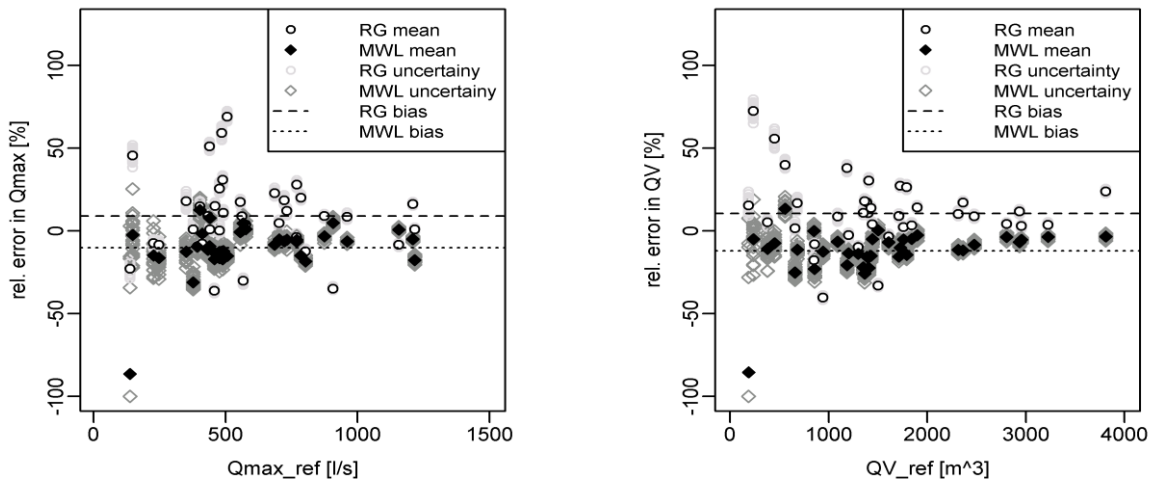

Figure 3 Relative error for different peak flows (left) and outflow volumes (right) expressed in percent.

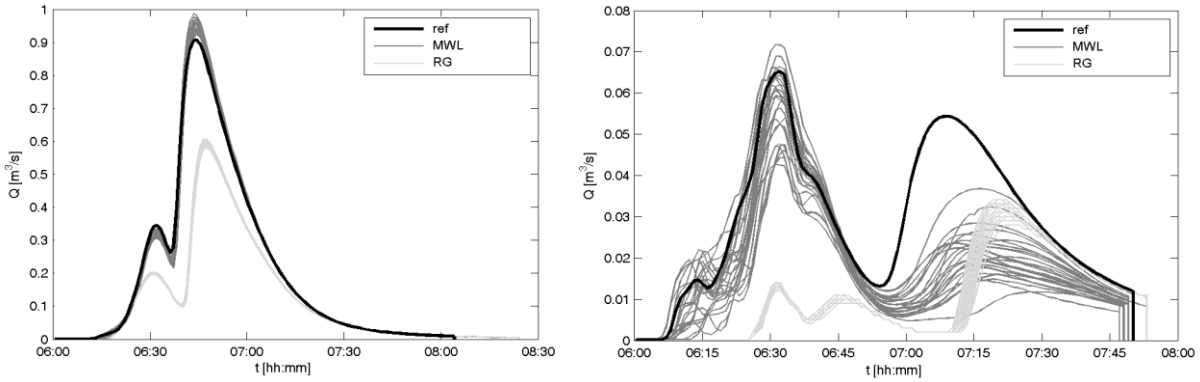

Figure 4 Outflow dynamics for periods of heavy (left) and light rainfall (right). The limited precision of MWL causes high relative deviations in MWL estimates, especially during light rainfall. However, in contrast to RG, MWL reflect the rainfall spatial variability and thus capture better the outflow dynamics.

Interestingly, the MWL perform better (considering NRMSE (6), CV(RMSE) (8) and correlation) when MWL hydrographs are shifted one minute backwards. On the other hand, the RG performs better when the RG series are not shifted or (considering CV(RMSE) (8)) when shifted one minute forward. This is probably caused by rainfalls coming from the east, where the density of the MWL is lower and rainfall reaches the RG first. In addition, the eastern part of the catchment has a high percentage of impervious areas, and since it is relatively close to the outfall of the catchment this influences the outflow dynamics considerably. However, a comparison of MWL and RG observations clearly shows that the MWL generally perform better than RG, despite temporal shifting.

Table 3 Performance statistics of estimated flow course to the reference one. The average values of particular measures over entire events and realizations are shown. The standard deviation is given in brackets.

Time shift [min]		-2	-1	0	1	2
NMAE [%]	RG	7.8 (5.8)	7.2 (6.1)	6.9 (6.3)	7 (6.5)	7.4 (6.5)
	MWL	5.5 (5.2)	4.9 (5.2)	4.8 (5.2)	5.2 (5)	6 (4.8)
NRMSE [%]	RG	13.9 (8.7)	12.8 (9.2)	12 (9.6)	11.9 (9.7)	12.4 (9.7)
	MWL	9 (7.9)	8.4 (8.1)	8.8 (8.2)	10.1 (7.8)	11.8 (7.5)
CV(MSE) [%]	RG	29.4 (16.1)	26.8 (16.9)	25.5 (17.8)	25.9 (18.1)	27.5 (18)
	MWL	20.5 (16.9)	18.3 (17.4)	17.7 (17.5)	19.4 (16.8)	22.8 (16)
CV(RMSE) [%]	RG	54.5 (29.9)	49.5 (30.1)	46.1 (30.4)	45.3 (29.9)	47.3 (29)
	MWL	34.9 (28.7)	32.2 (29.2)	33.6 (29.2)	39.1 (28.1)	46 (27.2)
corr. [-]	RG	0.931 (0.099)	0.939 (0.106)	0.942 (0.114)	0.94 (0.123)	0.933 (0.132)
	MWL	0.972 (0.064)	0.975 (0.065)	0.971 (0.067)	0.96 (0.069)	0.945 (0.073)

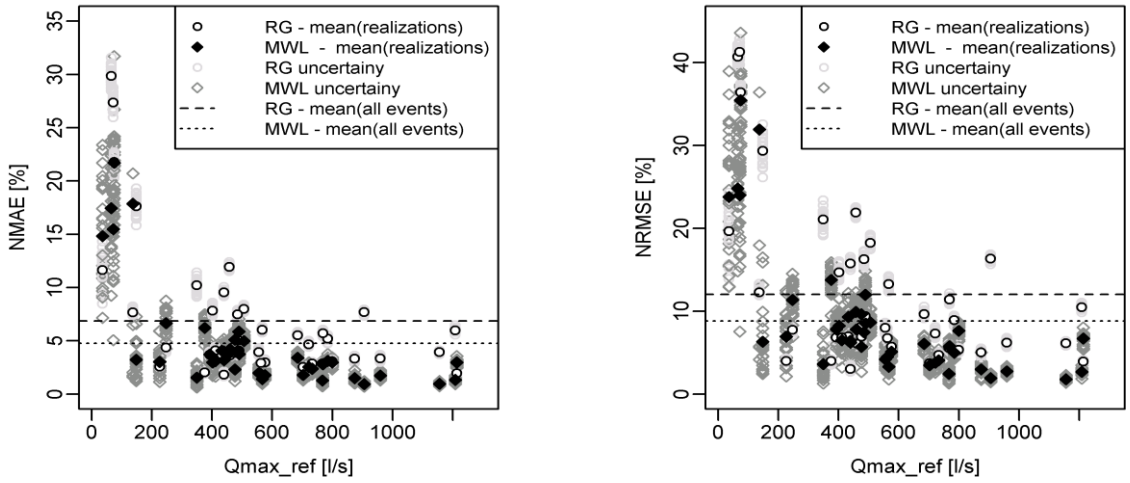

Figure 5 NMAE (left) and NRMSE (right) for different peak flows expressed in percent.

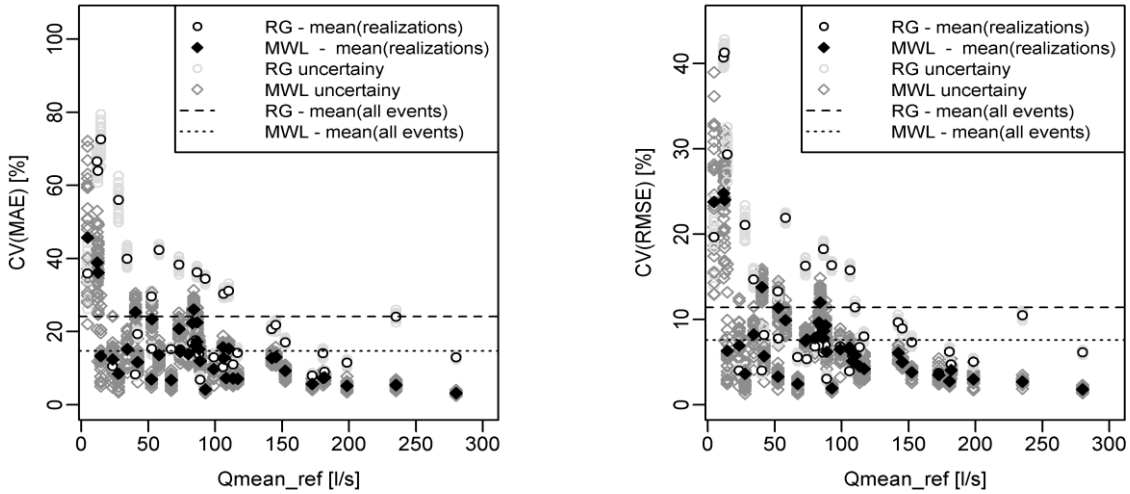

Figure 6 CV(MAE) (left) and CV(RMSE) (right) for different mean flows expressed in percent.

Although we took great efforts to assess measurement uncertainties, our results do not yet include the effect of antenna wetting for the MWL observations because this is still subject to ongoing research (Schleiss 2013). Based on our current understanding of the phenomenon we can speculate that, on the one hand, antenna wetting might increase both systematic and random observation errors, especially during heavy rainfall. On the other hand, MWL networks are often extremely dense in urban areas, which should allow us to improve the accuracy of MWL observations by considering observations from many links, which should contain redundant information.

CONCLUSION

In our study, we found that better information from telecommunication microwave links on spatio-temporal rainfall variability has the potential to improve pipe flow predictions compared with those from RG observations. Our results show that, first, MWL rainfall reconstruction smoothes out the local maxima and minima due to the path-averaged observations. Interestingly, although MWL observations have this bias, we found, second, that they very well reproduce areal averaged rain rates. Third, they reproduce the runoff dynamics better than point RG measurements, which simply lack the spatial rainfall information. This is especially important for urban hydrological applications because the reliability of point measurements is especially low for heavy convective rainfall with its high spatial variability. Fourth, we find that runoff from MWL observations better reproduce the rising branch of the runoff hydrograph. This is because they can capture rain rates over the whole area of the catchment and thus better observe the onset of precipitation. Regarding urban drainage applications, this could greatly improve the real time control of drainage systems. In the future, the MWL could nicely complement existing RG point measurements with the missing spatial rainfall information. This could constitute an important contribution to improve discharge predictions through better input data and also improve the control of the discharges from urban areas.

ACKNOWLEDGEMENTS

This work was supported by the project of Czech Technical University in Prague project no. SGS12/045/OHK1/1T/11, SGS13/127/OHK1/2T/11 and the European Union, OP RDI project No. CZ.1.05/2.1.00/03.0091 – University Centre for Energy Efficient Buildings. Further, we would like to thank T-Mobile Czech Republic a.s. for kindly providing us with information on the MWL network. The Prazska Vodohospodarska spolecnost a.s. is acknowledged for providing us with their hydrodynamic model. People from Prazske vodovody a kanalizace, a.s. were very helpful in selecting the appropriate case study area. Last but not least we would also like to thank the employees of Sweco Hydroprojekt a.s. and DHI a.s. for consulting regarding the rainfall-runoff model.

LIST OF REFERENCES

Beard, K. V. 1977 Terminal velocity adjustments for cloud and precipitation drops aloft. *Journal of Atmospheric Sciences* 34, 1293–1298

Berne, A., G. Delrieu, J.D. Creutin, and C. Obled 2004 Temporal and spatial resolution of rainfall measurements required for urban hydrology. *Journal of Hydrology* 299, 166-179.

Berne A. and R. Uijlenhoet 2007 Path-averaged rainfall estimation using microwave links: Uncertainty due to spatial rainfall variability. *Geophysical Research Letters* 34, L07403

Fenicia, F., L. Pfister, D. Kavetski, P. Matgen, J.-F. Iffy, L. Hoffmann, and R. Uijlenhoet 2012 Microwave links for rainfall estimation in an urban environment: Insights from an experimental setup in Luxembourg-city. *Journal of Hydrology* 464-465, 69-78.
Fencl, M., (2011). Reducing the uncertainty in rainfall-runoff modelling using commercial microwave links, Master's Thesis, Department of Sanitary and Ecological Engineering, Czech Technical University in Prague, Czech Republic.
Goldshtein, O., H. Messer, and A. Zinevich 2009 Rain rate estimation using measurements from commercial telecommunications links. *Signal Processing, IEEE Transactions* 57, 1616-1625.
Kharadly, M. M. Z., and R. Ross. 2001 Effect of wet antenna attenuation on propagation data statistics. *IEEE Transactions on Antennas and Propagation* 49 (8), 1183–1191.
Leijnse, H., R. Uijlenhoet, and J. N. M. Stricker 2007 Rainfall measurement using radio links from cellular communication networks. *Water Resources Research* 43 (3), W03201.
Leijnse, H., R. Uijlenhoet, and J. N. M. Stricker 2008 Microwave link rainfall estimation: Effects of link length and frequency, temporal sampling, power resolution, and wet antenna attenuation. *Advances in Water Resources* 31, 1481–1493
Messer, H., A Zinevich, and P. Alpert 2006 Environmental Monitoring by Wireless Communication Networks. *Science* 312, 713-713.
Mishchenko, M. I. and L.D. Travis 1998 Capabilities and limitations of a current FORTRAN implementation of the T-matrix method for randomly oriented, rotationally symmetric scatterers. *Journal of Quantitative Spectroscopy and Radiative Transfer* 60(3), 309-324.
Overeem, A., H. Leijnse, and R. Uijlenhoet 2011 Measuring urban rainfall using microwave links from commercial cellular communication networks. *Water Resources Research* 47, W12505.
Rieckermann J., R. Lüscher and S. Krämer 2009 Assessing Urban Precipitation using Radio Signals from a Commercial Communication Network. In: *8th International Workshop on Precipitation in Urban Areas*, 10-13 December, 2009, St. Moritz, Switzerland.
Schleiss, M., J. Jaffrain and A. Berne 2012 Stochastic simulation of intermittent DSD fields in time. *Journal of Hydrometeorology* 13(2), 621-637.
Schleiss, M., J. Rieckermann, and A. Berne 2013 Quantification and modeling of wet-antenna attenuation for commercial microwave links. *IEEE Geosci. Remote Sens. Lett.*, in press.
Schleiss, M., Rieckermann, J., Berne, A., 2013. Quantification and Modeling of Wet-Antenna Attenuation for Commercial Microwave Links. *IEEE Geoscience and Remote Sensing Letters Early Access Online*.
Sevruk, B. 1996 Adjustment of tipping-bucket precipitation gauge measurement. *Atmospheric Research* 42, 237-246.
Stransky D., V. Bares and P. Fatka 2007 The effect of rainfall measurement uncertainties on rainfall-runoff processes modelling. *Water Science and Technology* 55(4), 103-111.
Thorndahl, S. and M.R. Rasmussen 2012 Marine X-band weather radar data calibration. *Atmospheric Research* 103, 33-44.